PART 4

GEOPHYSICAL SURVEY BY USING ELECTRICAL RESISTIVITY TECHNIQUE

EXCUTIVE SUMMARY

Electrical resistivity method is one of the geophysics subsurface exploration techniques used to determine subsurface profile characteristics and groundwater occurrence. This method was performed to evaluate the dam seepage characteristics at Semberong dam. Eight lines of electrical resistivity survey were conducted using ABEM Terrameter LS-2 combined with four electrode cables. Resistivity data processing was performed using RES2DINV software for calculating resistivity configuration data input and generating 2D image of subsurface profile within the study area based on electrical resistivity distribution. Results verification were successfully done through the correlation of resistivity data based on site observation. It was found that the low resistivity values range from 10 to 150 ohm.m were indicated in resistivity images especially in L1-L1', L2-L2', L6-L6', L7-L7' and L8-L8' profiles can be defined as the presence of permeable soils saturated with water. It was believed the presence of saturated water in dam embankment that caused the problem of water seepage and these results are in line with the locations of these water seepage occurring in the southern part of the study.

Occurrence of water zone more dominantly at south of study area compared to north area that facing water dam. There are two possible causes of water seepage dams occur. First due to the high-pressure head subsequently induced high pore water pressure and the pressure is released at the seepage points especially in the boundary connection area between engineered material dam and natural material dam. The pressure results in collapsed and eroded soil block that occurs in the area resulting in seepage drainage. The second cause is due to excessive agriculture irrigation activity that acts from the surrounding of the embankment dam.

However, further investigation such as using borehole data may be able to confirm in detail regarding the groundwater seepage from electrical resistivity method within this area. The propose remediation action can be used by constructing a few numbers of withdrawal tube wells for reducing groundwater level at acceptable limit within this area.

RINGKASAN EKSEKUTIF

Kaedah keberintangan elektrik adalah salah satu kaedah geofizik bagi penyiasatan penyaisatan tanah bawah permukaan yang digunakan untuk menentukan ciri profil bawah permukaan dan air bawah tanah. Kaedah ini dilakukan untuk menilai kejadian air rembesan yang berlaku di empangan Semberong. Lapan garisan imbasan keberintangan elektrik dilakukan menggunakan ABEM Terrameter LS-2 yang digabungkan dengan empat kabel elektrod. Pemprosesan data kerintangan dilakukan menggunakan perisian RES2DINV untuk mengira input data konfigurasi kerintangan dan menghasilkan gambar 2D profil bawah permukaan dalam kawasan kajian berdasarkan taburan keberintangan elektrik. Pengesahan hasil berjaya dilakukan melalui korelasi data kerintangan berdasarkan pemerhatian dilapangan. Didapati bahawa nilai keberintangan elektrik rendah berjulat antara 10 hingga 150 ohm.m ditunjukkan dalam imej keberintangan elektrik terutamanya dalam profil L1-L1 ', L2-L2', L6-L6', L7-L7 'dan L8-L8' dapat didefinisikan sebagai kehadiran material tanah yang telap tepu dengan air. Dipercayai kehadiran air tepu di dalam tambakan empangan menyebabkan masalah rembesan air. Kehadiran zon air lebih dominan di selatan kawasan kajian berbanding dengan kawasan utara yang menghadapi empangan air dan keputusan in selari dengan lokasi-lokasi rembesan ini berlaku di bahagian selatan kajian. Terdapat dua kemungkinan punca rembesan air berlaku. Pertama disebabkan oleh tekanan turus yang tinggi dan secara tak langsung menaikkan tekanan air rongga yang tinggi dan tekanan itu dilepaskan di titik-titik rembesan terutamanya di kawasan sambungan sempadan antara "engineered" material empangan dan "natural" material empangan. Tekanan tersebut mengakibatkan runtuhan and hakisan blok tanah yang berlaku di kawasan tersebut yang menghasilkan saliran rembesan. Punca kedua adalah disebabkan oleh kegiatan saliran yang berlebihan dari arah belakang empangan tambakan tersebut. Walau bagaimanapun, penyiasatan lebih lanjut seperti menggunakan data lubang jara mungkin dapat mengesahkan secara terperinci mengenai rembesan air bawah tanah. Usulan tindakan pemulihan jangka pendek boleh dilakukan dengan membina sejumlah telaga tiub untuk dipam bagi mengurangkan paras air bawah tanah di kawasan ini pada tahap yang dibenarkan.

DAM SEEPAGE STUDY AT SEMBERONG DAM JOHORE BY USING ELECTRICAL RESISTIVITY

4.1 Introduction

The Sembrong Dam form part of a larger scheme, namely the Western lohor Agricultural Development Project. It was undertaken by the Drainage and Irrigation Department (DID) mainly for flood mitigation, the dam was also utilized for water supply purposes by the Syarikat Air Johor (SAJ).

In November 2018, there was an observation from the DID staffs that identified the movement of soil and the occurrence of sinkholes as a result of water seepage releases from the main embankment dam at the location CH1850. Therefore, a series of discussions and site visits were conducted by RECESS together with DID and the relevant agencies to investigate and indirectly mitigate this problem. One of the method investigation study suggested is geophysical study.

Geophysical study was used for determining the causes of seepage at Semberong dam Air Hitam, Johor Darul Takzim. Electrical Resistivity Method (ERM) was used in this study as requested by Department Irrigation and Drainage (DID) to determine the subsurface profile condition within this area. This method can determine the presence of soil lithology, bedrock, groundwater and boulders (Mohd Hazreek et. al, 2011) in order to assess the causes of dam seepage. The geo-electrical method indirectly compliments the conventional method such as borehole information, in order to correlate the lithology information and groundwater occurrence. Furthermore, this method is more cost effective for subsurface investigations.

4.2 Scopes of work

The ERM was carried out involved two-dimensional (2-D) imaging resistivity survey. The transverse survey distance was ranges about 80m which depend on the space provided in undulating area that was not more than 45 degree. The Wenner-Schlumberger configuration was chosen based on space provided in flat area and the depth of penetration interest in order to identify the presence of subsurface lithologies and groundwater occurrence. **EIGHT (8)** resistivity survey lines (Figure 4.1) were conducted at parallel and perpendicular orientation within study area.

Figure 4.1: Location of electrical resistivity survey lines

4.3 Study Area

The study area is located at the Semberong dam which is nearby with Air Hitam town. The distance between the study area and Air Hitam town is about 1.3 km. The exact location of the area was at longitudes E 103.909683° to E 103.912880° and latitudes N 1.523570° to N 1.524549°. From observation, topographic of the area showed that it was undulating area. The catchment spans across two districts, i.e. Batu Pahat on the western side, and Kluang on the east. Sembrong basin sits cusped in three administrative districts, i.e. Majlis Daerah Kluang, Majlis Daerah Batu Pahat and Majlis Daerah Yong Peng.

4.4 Coordinates and Reduced Level of Resistivity Survey

The exact locations, namely longitude and latitude of the transverse survey points were determined in the field with the help of Global Positioning System (GPS), Garmin Etrex Model and Unmanned Automatic Vehicle (UAV) drone. The horizontal accuracy of GPS is nearly 3-4m when the strong satellite signals were detected. Tables 4.1, 4.2, 4.3 and 4.4 showed the coordinates measured from transverse survey labeled. To locate the high topographical form of dam ground, aerial images are used to construct the contour of elevation (N, Elliposid height). The Agisoft PhotoScan can align essential 2D model point after all the image information has been synchronized. The 2D model was built with 120 camera stations and 378 646 tie projections. Then all the point clouds are used to build dense point cloud. Next step is to construct the dense point cloud to mesh the 2D map together, producing a shaded model form. Textured model will generate a smooth texture of full 3D model. Figure 4.2 shows full elevation and generation of textured model at study area.

Figure 4.2: Elevation and generation of textured model

4.5 Geology and Hydrogeology

According to the geological map produced by Department of Mineral and Geoscience Malaysia (DMGM) in 1985, the study area was located in alluvium Quaternary sediment deposits especially along the Sembrong River. The Quaternary sediment covered the surface of study area was overlain and surrounded by sedimentary rock that probably consist of interbedded Shale and Sandstone type under Gemas Formation (Figure 4.3). In general, the presence of this type of rock exhibits fractured geology structures, namely faults and joints. The fractures from these structures provided surface water seepage to underground, groundwater carriage, and water storage in rock formation. Subsequently, this process encouraged weathering process of geologic materials encountered in this area extensively.

Table 4.1: Coordinates and Reduced Levels of Electrical Resistivity Survey for Lines 1 and 2

ID No.	Distance (m)	North°	Easting°	Reduced level (m.msl)	ID No.	Distance (m)	North°	Easting°	Reduced level (m.msl)
1/L1	0.00	1°58'39.81"	103°10'29.36"	18.850	1/L2	0.00	1°58'40.33"	103°10'29.29"	20.440
2	5.00	1° 58' 40"	103° 10' 30"	18.540	2	5.00	1°58'40.25"	103°10'29.45"	20.350
3	10.00	1°58'39.73"	103°10'29.71"	18.500	3	10.00	1°58'40.20"	103°10'29.59"	20.200
4	15.00	1°58'39.69"	103°10'29.86"	18.100	4	15.00	1°58'40.14"	103°10'29.74"	20.540
5/LL1	20.00	1°58'39.67"	103°10'30.03"	17.550	5/LL2	20.00	1°58'40.06"	103°10'29.88"	20.650
6	25.00	1°58'39.63"	103°10'30.18"	17.240	6	25.00	1°58'40.03"	103°10'30.01"	20.100
7	30.00	1°58'39.58"	103°10'30.32"	16.660	7	30.00	1°58'39.99"	103°10'30.17"	20.050
8	35.00	1°58'39.54"	103°10'30.44"	15.720	8	35.00	1°58'39.95"	103°10'30.32"	19.970
9/CP1	40.00	1°58'39.46"	103°10'30.61"	15.600	9/CP2	40.00	1°58'39.91"	103.175127°	19.760
10	45.00	1°58'39.42"	103°10'30.76"	15.500	10	45.00	1°58'39.89"	103°10'30.61"	19.200
11	50.00	1°58'39.38"	103°10'30.92"	15.340	11	50.00	1°58'39.87"	103°10'30.74"	19.400
12	55.00	1°58'39.34"	103°10'31.08"	15.840	12	55.00	1°58'39.85"	103°10'30.92"	18.300
13/LR1	60.00	1°58'39.31"	103°10'31.23"	15.900	13/LR2	60.00	1°58'39.80"	103°10'30.99"	17.620
14	65.00	1°58'39.28"	103°10'31.34"	15.820	14	65.00	1°58'39.78"	103°10'31.44"	17.400
15	70.00	1°58'39.26"	103°10'31.49"	15.940	15	70.00	1°58'39.74"	103°10'31.58"	17.650
16	75.00	1°58'39.23"	103°10'31.63"	15.950	16	75.00	1°58'39.72"	103°10'31.74"	17.550
17/L1'	80.00	1°58'39.21"	103°10'31.81"	16.168	17/L2'	80.00	1°58'39.68"	103°10'31.64"	17.630

Table 4.2: Coordinates and Reduced Levels of Electrical Resistivity Survey for Lines 3 and 4

ID No.	Distance (m)	North°	Easting°	Reduced level (m.msl)	ID No.	Distance (m)	North	Easting	Reduced level (m.msl)
1/L3	0.00	1°58'40.97"	103°10'29.22"	22.020	1/L4	0.00	1°58'42.48"	103°10'29.18"	21.690
2	5.00	1°58'40.92"	103°10'29.34"	22.010	2	5.00	1°58'42.41"	103°10'29.24"	21.500
3	10.00	1°58'40.88"	103°10'29.47"	21.950	3	10.00	1°58'42.36"	103°10'29.35"	21.400
4	15.00	1°58'40.84"	103°10'29.64"	22.300	4	15.00	1°58'42.26"	103°10'29.48"	21.670
5/LL3	20.00	1°58'40.80"	103°10'29.80"	21.850	21.795	20.00	1°58'42.16"	103°10'29.59"	21.580
6	25.00	1°58'40.73"	103°10'29.95"	21.800	6	25.00	1°58'42.08"	103°10'29.76"	21.400
7	30.00	1°58'40.70"	103°10'30.08"	21.670	7	30.00	1°58'41.97"	103°10'29.91"	21.500
8	35.00	1°58'40.64"	103°10'30.24"	21.580	8	35.00	1°58'41.91"	103°10'30.07"	20.980
9/CP3	40.00	1°58'40.60"	103°10'30.44"	21.540	9/CP4	40.00	1°58'41.85"	103°10'30.23"	20.260
10	45.00	1°58'40.57"	103°10'30.57"	22.010	10	45.00	1°58'41.82"	103°10'30.44"	20.540
11	50.00	1°58'40.58"	103°10'30.73"	22.350	11	50.00	1°58'41.79"	103°10'30.63"	20.750
12	55.00	1°58'40.59"	103°10'30.89"	22.150	12	55.00	1°58'41.78"	103°10'30.82"	20.650
13/LR3	60.00	1°58'40.55"	103°10'30.98"	22.150	13	60.00	1°58'41.76"	103°10'30.97"	20.813
14	65.00	1°58'40.52"	103°10'31.20"	22.600	14	65.00	1°58'41.72"	103°10'31.14"	20.410
15	70.00	1°58'40.44"	103°10'31.34"	22.400	15	70.00	1°58'41.66"	103°10'31.32"	20.650
16	75.00	1°58'40.37"	103°10'31.51"	22.350	16	75.00	1°58'41.55"	103°10'31.44"	20.765
17/L3'	80.00	1°58'40.30"	103°10'31.44"	22.290	17/L4'	80.00	1°58'41.43"	103°10'31.54"	20.933

Table 4.3: Coordinates and Reduced Levels of Electrical Resistivity Survey for Lines 5 and 6

ID No.	Distance (m)	North	Easting	Reduced level (m.msl)	ID No.	Distance (m)	North	Easting	Reduced level (m.msl)
1/L5	0.00	1°58'42.96"	103°10'29.32"	21.570	1/L6	0.00	1°58'38.69"	103°10'29.26"	14.980
2	5.00	1°58'42.81"	103°10'29.43"	21.220	2	5.00	1°58'38.64"	103°10'29.41"	15.100
3	10.00	1°58'42.67"	103°10'29.56"	20.950	3	10.00	1°58'38.58"	103°10'29.61"	15.300
4	15.00	1°58'42.55"	103°10'29.67"	20.750	4	15.00	1°58'38.51"	103°10'29.77"	15.200
5/LL5	20.00	1°58'42.45"	103°10'29.77"	20.640	5/LL6	20.00	1°58'38.46"	103°10'29.93"	15.140
6	25.00	1°58'42.33	103°10'29.89"	20.450	6	25.00	1°58'38.40"	103°10'30.10"	15.450
7	30.00	1°58'42.26"	103°10'30.05"	20.440	7	30.00	1°58'38.37"	103°10'30.25"	15.320
8	35.00	1°58'42.17"	103°10'30.19"	20.600	8	35.00	1°58'38.35"	103°10'30.44"	15.10
9/CP5	40.00	1°58'42.10"	103°10'30.29"	20.304	9/CP6	40.00	1°58'38.30"	103°10'30.76"	15.106
10	45.00	1°58'42.03"	103°10'30.49"	20.400	10	45.00	1°58'38.28"	103°10'30.91"	15.045
11	50.00	1°58'41.96"	103°10'30.64"	21.400	11	50.00	1°58'38.23"	103°10'31.09"	15.070
12	55.00	1°58'41.91"	103°10'30.80"	20.750	12	55.00	1°58'38.20"	103°10'31.22"	14.917
13/LR5	60.00	1°58'41.88"	103°10'30.90"	20.590	13/LR6	60.00	1°58'38.17"	103°10'31.43"	15.102
14	65.00	1°58'41.85"	103°10'31.12"	20.950	14	65.00	1°58'38.13"	103°10'31.58"	15.140
15	70.00	1°58'41.83"	103°10'31.27"	20.950	15	70.00	1°58'38.12"	103°10'31.71"	15.157
16	75.00	1°58'41.82"	103°10'31.40"	21.020	16	75.00	1°58'38.11"	103°10'31.88"	15.165
517/L5'	80.00	1°58'41.80"	103°10'31.37"	21.021	17/L6'	80.00	1°58'38.11"	103°10'31.97"	15.170

Table 4.4: Coordinates and Reduced Levels of Electrical Resistivity Survey for Lines 7 and 8

ID No.	Distance (m)	North°	Easting°	Reduced level (m.msl)	ID No.	Distance (m)	North	Easting	Reduced level (m.msl)
1/L7	0.00	1°58'39.10"	103°10'29.56"	17.680	1/L8	0.00	1°58'40.74"	103°10'30.28"	24.220
2	5.00	1°58'39.00"	103°10'29.66"	17.500	2	5.00	1°58'40.64"	103°10'30.33"	23.750
3	10.00	1°58'38.97"	103°10'29.83"	17.550	3	10.00	1°58'40.49"	103°10'30.39"	22.250
4	15.00	1°58'38.93"	103°10'30.00"	17.580	4	15.00	1°58'40.33"	103°10'30.45"	21.880
5/LL7	20.00	1°58'38.92"	103°10'30.27"	17.470	5/LL8	20.00	1°58'40.20"	103°10'30.48"	20.160
6	25.00	1°58'38.91"	103°10'30.39"	16.950	6	25.00	1°58'39.99"	103°10'30.50"	18.450
7	30.00	1°58'38.91"	103°10'30.59"	16.720	7	30.00	1°58'39.84"	103°10'30.48"	17.500
8	35.00	1°58'38.92"	103°10'30.73"	15.950	8	35.00	1°58'39.63"	103°10'30.46"	16.500
9/CP7	40.00	1°58'38.88"	103°10'30.93"	15.235	9/CP8	40.00	1°58'39.43"	103°10'30.46"	16.120
10	45.00	1°58'38.86"	103°10'31.05"	15.200	10	45.00	1°58'39.29"	103°10'30.45"	16.100
11	50.00	1°58'38.81"	103°10'31.23"	15.100	11	50.00	1°58'39.09"	103°10'30.44"	15.600
12	55.00	1°58'38.76"	103°10'31.41"	15.050	12	55.00	1°58'39.00"	103°10'30.46"	15.276
13/LR7	60.00	1°58'38.70"	103°10'31.61"	14.964	13/LR8	60.00	1°58'38.69"	103°10'30.48"	15.250
14	65.00	1°58'38.66"	103°10'31.72"	15.100	14	65.00	1°58'38.53"	103°10'30.52"	15.180
15	70.00	1°58'38.60"	103°10'31.92"	15.106	15	70.00	1°58'38.37"	103°10'30.56"	15.150
16	75.00	1°58'38.56"	103°10'31.98"	15.109	16	75.00	1°58'38.27"	103°10'30.59"	15.100
17/L7'	80.00	1°58'38.50"	103°10'31.99"	15.208	17/L8'	80.00	1°58'38.17"	103°10'30.66"	15.030

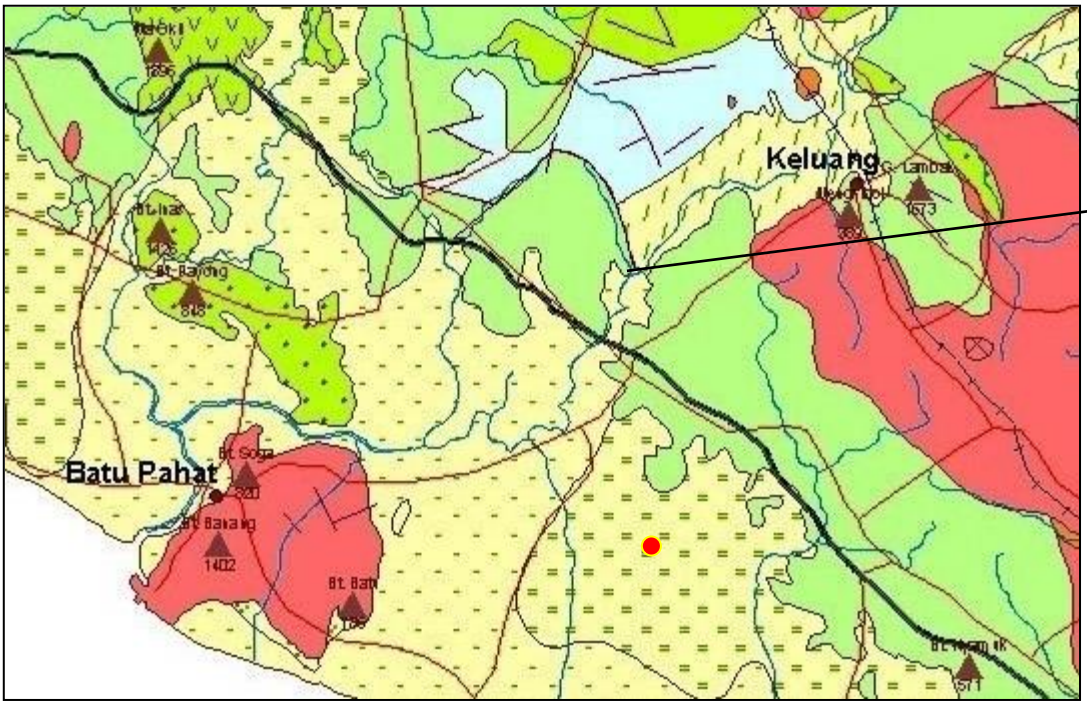

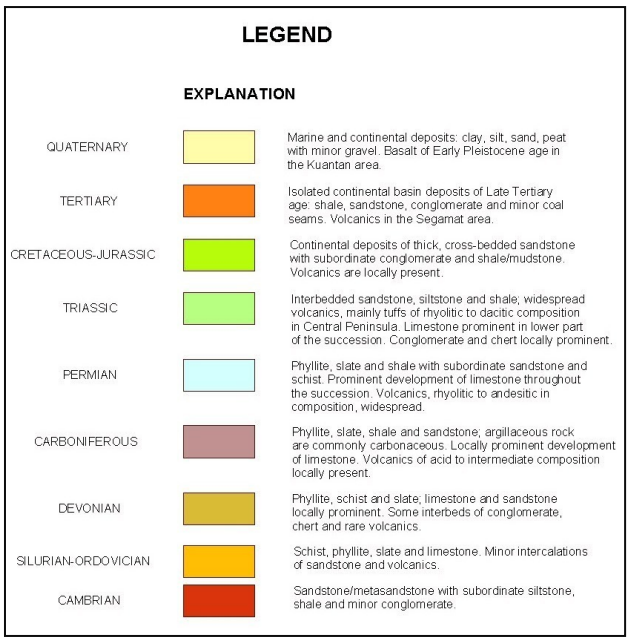

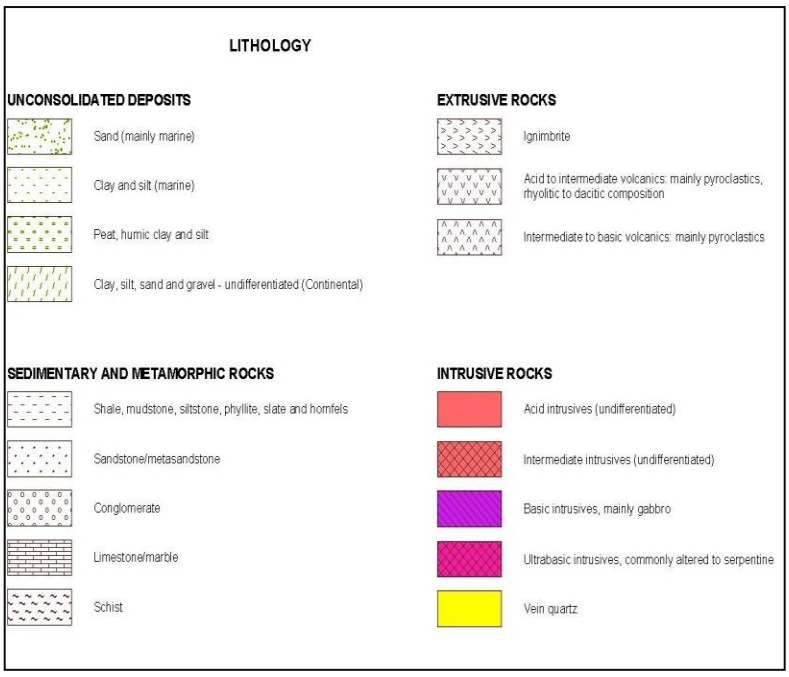

Figure 4.3: The Geology of the study area (DMGM, 1985)

4.6 Methodology

Resistivity traverses were performed on 26th November until 27th November 2020. The resistivity survey was conducted using the ABEM LS-2, combined with accessories of equipment. **EIGHT (8)** resistivity image profiles (L1 to L1', L2 to L2', L3 to L3', L4 to L4', L5 to L5', L6 to L6', L7 to L7' and L8 to L8' (see Figure 4.1) were measured across the area. For each profile, 61 electrodes were peg into the ground surface at the site. The survey traverses were oriented at N-S and W-E. The Wenner-Schlumberger array was used in this work. This array was chosen for the resistivity traverses because it gives a dense near-surface and deeper cover of resistivity data. Also, the array provides a good vertical resolution and can give a clear image of groundwater and sand-clay boundaries as horizontal structures (Hamzah et.al, 2006). The array was used for short distance of spacing in the area.

The data gathered in this survey were interpreted through the RES2DINV software of Loke et al. (2003) to provide an inverse model that approximates the actual subsurface structure. To obtain the resistivity section, the inversion algorithm, RES2DINV was used to process the data, as proposed by Loke and Barker (1996). The inversion routine used by the program RES2DINV was based on the smooth constrained method. This program divides the two-dimensional model used in the subsurface into a number of rectangular blocks (Loke and Barker 1996). To minimize the difference between the measured and the calculated apparent resistivity values, the resistivity of the blocks was adjusted iteratively. The latter was calculated by the finite-difference method of Dey and Morrison (1979). Resistivity field data collected through the Wenner-Schlumberger array from individual survey lines were inverted individually to generate a two-dimensional Wenner-Schlumberger resistivity model. The inversions were performed on an AMD Athlon(tm) 64 X2 Dual-Core Proceessor TK-57 1.90GHz with 3.00GB of RAM. An initial model was produced, from which a response was calculated and compared to the measured data. The starting model was then modified in such a way as to reduce the differences between the model response and the measured data. The differences were quantified as root-mean-squared (RMS) errors. This process continues iteratively until the RMS error falls within acceptable limits, usually below 10%, or until the change between RMS values calculated for consecutive iterations becomes insignificant (Awni, 2006). The model with the lowest possible RMS errors, however, was not always the most appropriate one as it can show unrealistic variations in the resistivity model (Loke, 2000). Finite difference method was used as the data includes topography.

Table 4.5 showed the resistivity values of common rocks, soil materials and chemicals. The resistivity of these rocks was greatly dependent on the degree of fracturing, and the percentage of the fractures filled with groundwater. Sedimentary rocks, which usually are more porous and have higher water content, normally have lower resistivity values. Wet soils and fresh groundwater have even lower resistivity values. Clayey soil normally has a lower resistivity value than sandy soil. However, note the overlap in the resistivity values of the different classes of rocks

and soils. This is because the resistivity of a particular rock and soil sample depends on a number of factors such as the porosity, the degree of water saturation and the concentration of dissolved salts.

Table 4.5: Resistivities of some common rocks, minerals and chemicals (Keller and Frishcknecht 1996, Daniels and Alberty 1996 and Loke 1999)

Material	**Resistivity** ($\Omega.m$)	**Conductivity (Siemen/m)**
Igneous and Metamorphic rocks		
Granite	$5x10^3$-10^6	10^{-6}-$2x10^{-4}$
Basalt	10^3-10^6	10^{-6}-10^{-3}
Slate	$6x10^2$-$4x10^7$	$2.5x10^{-8}$-$1.7x10^{-3}$
Marble	10^2-$2.5x10^8$	$4x10^{-9}$-10^{-2}
Quarzite	10^2-$2x10^8$	$5x10^{-9}$-10^{-2}
Schist	50-10^4	$2x10^{-2}$-10^{-4}
Hornfels	$8x10^3$-$6x10^7$	$1.7x10^{-8}$-$1.3x10^{-4}$
Sedimentary rocks		
Sandstone	8-$4x10^3$	$2.5x10^{-4}$-0.125
Shale	20-$2x10^3$	$5x10^{-4}$-0.05
Limestone	50-$4x10^2$	$2.5x10^{-3}$-0.02
Soils and water		
Clay	1-100	0.01-1
Alluvium	10-800	$1.25x10^{-3}$-0.1
Groundwater (Fresh)	10-100	0.01-0.1
Seawater	0.2	5

4.7 Results of investigation and Interpretations

EIGHT (8) profiles of 2-D electrical resistivity distribution were obtained from the surveys were carried out as shown in Figures 4.4, 4.5, 4.6, 4.7, 4.8, 4.9, 4.10 and 4.11. The labeled cross section of the profile was showed in Figures 4.1. The length of the survey lines is 80 m and depth of penetration ranges 20 to 25 m. Three color codes (red, green, and blue) are used to denote the different geologic materials as representative in an electrical resistivity model (Figures 4.4, 4.5, 4.6, 4.7, 4.8, 4.9, 4.10 and 4.11). The summary of electrical resistivity distribution as indicated in color codes versus material used in this study is shown in Table 4.6.

In general, the 2-D profile obtained from the electrical resistivity survey revealed three categories of geological materials (see in Figures 4.4, 4.5, 4.6, 4.7, 4.8, 4.9, 4.10 and 4.11);

a) Permeable soils saturated with water (possibly mixture of percolated water, groundwater sand and some clay and silt materials) showed the resistivity value ranges in between 10 to 150 ohm.m
b) Semipermeable soils materials (possible mixture of pore water, sand, clay and silt) showed the resistivity value ranges in between 200 to 1000 ohm.m
c) Impermeable soils materials (possible mixture of pore water, sand, clay and silt) showed the resistivity value ranges in between 1000 to 3,000 ohm.m.

Resistivity survey line L1-L1' located parallel at the back of the dam embankment (Figure 4.1) The resistivity image for the L1-L1' showed low resistivity values range between 10 to 150 ohm.m especially in the area of seepage points (S1 / S2) (Figure 4.4). It is believed that the low resistivity value shown in the seepage points is caused by the presence of high-pressure head occurs and followed to the equipotential line direction to the end of dam embankment. This pressure induced high pore water pressure and release by follow to natural seepage drainage created by pore water pressure to the seepage points. It is believed that the seepage occurred at the boundary connection area between the engineered material dam (right side) and the natural material dam (left side) from the center point (CP1) as shown in the image of resistivity line, L1-L1 '(Figure 4.4).

Resistivity survey line L2-L2' showed the boundary of the connection between the engineered material dam (right side) and natural material dam (left side) from the center point (CP2) where the high resistivity value (<1000 ohm.m) dominantly showed on the right side of the resistivity image. It is possible due to compacted materials engineered dam occurred at the right side compared to the left side which is a natural material dam by refer to the CP2 (Figures 4.1 and 4.5).

Resistivity survey line L3-L3' located near the crest embankment dam (Figure 4.1). The resistivity image indicated that there is a low resistivity value (10-150 ohm.m) presence at the engineered material dam (right side) of the resistivity image from CP3 (Figure 4.6). This is due to percolated water that occurred filling in the fracture space of the dam embankment. Photos in the appendix on lines L3-L3' showed that soil depression occurs in the area on dam surface and possible caused by due to the formation of cavities, sinkholes or cracks. The second possibility is due to the presence of chimney drain in the area which is a vertical waterway before going to the drainage blanket (horizontal).

Resistivity survey lines L4-L4 'and L5-L5' located parallel to the front of dam area (Figures 4.1, 4.6 and 4.7). Its showed that low resistivity values (10-150 ohm.m) occurred especially to the right side of the resistivity image at shallow depths (2-4 m) from ground surface level compared to the image of resistivity at the left side from the center points (CP4 and CP5) that across both survey lines. It is believed that the significant difference in resistivity value on the left and right sides of the resistivity images is the boundary of the connection between the engineered material dam (right side) and the natural material dam (left side).

Resistivity survey lines L6-L6 'and L7-L7' located behind the embankment dam and near the dam boundary area with the surrounding area (Figure 4.1). Low resistivity values (10-150 ohm.m) indicated in almost all images especially in the seepage point (S3) area. It is possible that the low resistivity value shown in the seepage point area is due to the presence of high-pressure head occurred and followed equipotential line which induced high pore water pressure. It is believed that the seepage occurred at the boundary connection area that occurred between the engineered material dam (right side) and the natural material dam (left side) from the center point (CP6) as shown at the L6-L6 'line resistivity image (Figure 4.8).

Resistivity survey line L8-L8' located at perpendicular with all lines (L1-L1' to L7-L7') and also crossed over the three seepage points (Figures 4.1 and 4.10). The resistivity image showed that there is a low resistivity value (10-150 ohm.m) encountered at a shallow depth (2-4 meters from the ground surface level) on the right side of the image which is located behind the dam and also the points of occurrence of seepage. It is possible that there is a collapsed and eroded soil block that occurs in the area that produces seepage drainage. It is due to the presence of high-pressure head occurs follow to the equipotential line which induces high pore water pressure and the pressure is released at the seepage points especially in the boundary area between the engineered material dam and natural material dam. The second possibility is due to the high table groundwater flow coming from surrounding area.

Low resistivity values (10-150 ohm.m) encountered at deeper depths (10-20m) on most resistivity survey images (L1-L1 ', L2-L2', L6-L6 ', L7-L7 'and L8-L8') which is most likely a dam foundation and interpreted as Shale rock or

clay saturated with water. Another possibility is that it is also a permeable geology material encountered consisting of sandstone rocks as described in the geology of the area covered by interbedded shale and sandstone.

The resistivity values range from 10 to 150 ohm.m were indicated in resistivity images especially in Figures 4.4, 4.5, 4.9, 4.10, and 4.11 can be defined as the presence of permeable soils saturated with water. It was believed the presence of saturated water in dam embankment had caused the problem of water seepage and these results are in line with the locations of these water seepage occurring in the southern part of the study. Occurrence of water zone more dominantly at south of study area compared to north area that facing water dam. The another causes of seepage, it is possible that a dam seepage occurs at the back of embankment that may have been caused by excessive watering agriculture irrigation near the dam area.

Resistivity value ranges in between 200 to 1,000 ohm.m showed in the all resistivity images profiles indicated that the presence of semipermeable soils materials (possible mixture of pore water, sand, clay and silt). Meanwhile resistivity value ranges from 1,000 to 3,000 ohm.m indicated the impermeable soils materials presence.

Table 4.6: Summary of resistivity value interpretation

No	Resistivity Value (Ωm)	Resistivity Legend	Interpretation
1	10~ 150	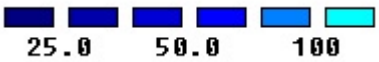	Permeable soils saturated with water (possibly mixture of soil water, groundwater, sand and some clay and silt materials)
2	200~1000		Semipermeable soils materials (possible mixture of pore water, sand, clay and silt)
2	1000 ~ 20000		Impermeable soils materials (possible mixture of pore water, sand, clay and silt)

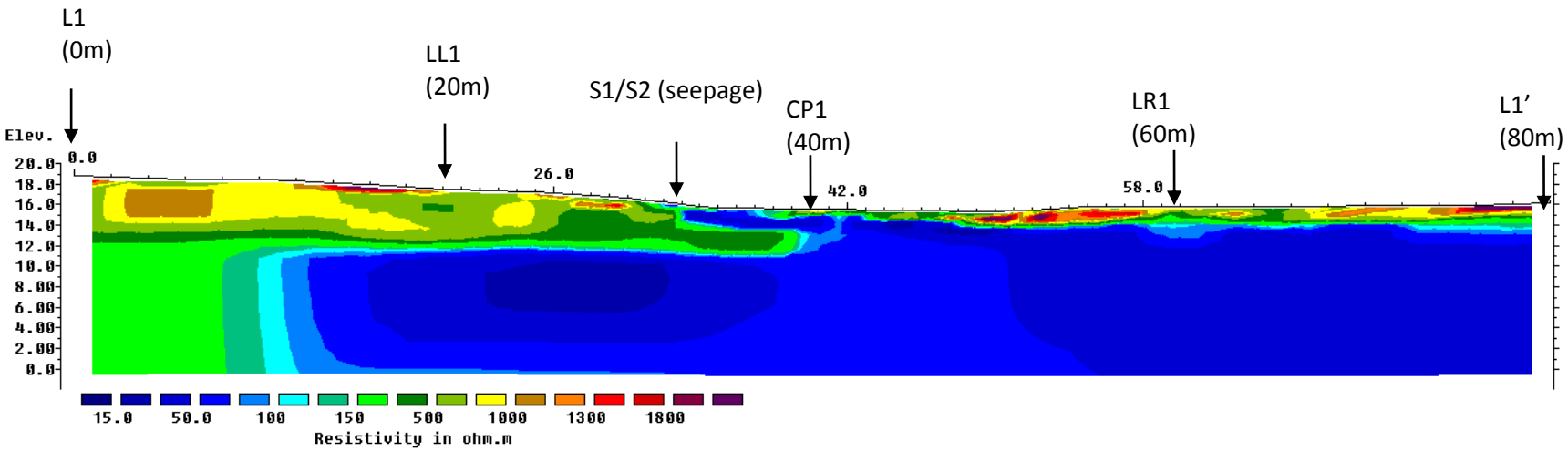

Figure 4.4: Subsurface image results by Electrical Resistivity method at line 1 (L1-L1')

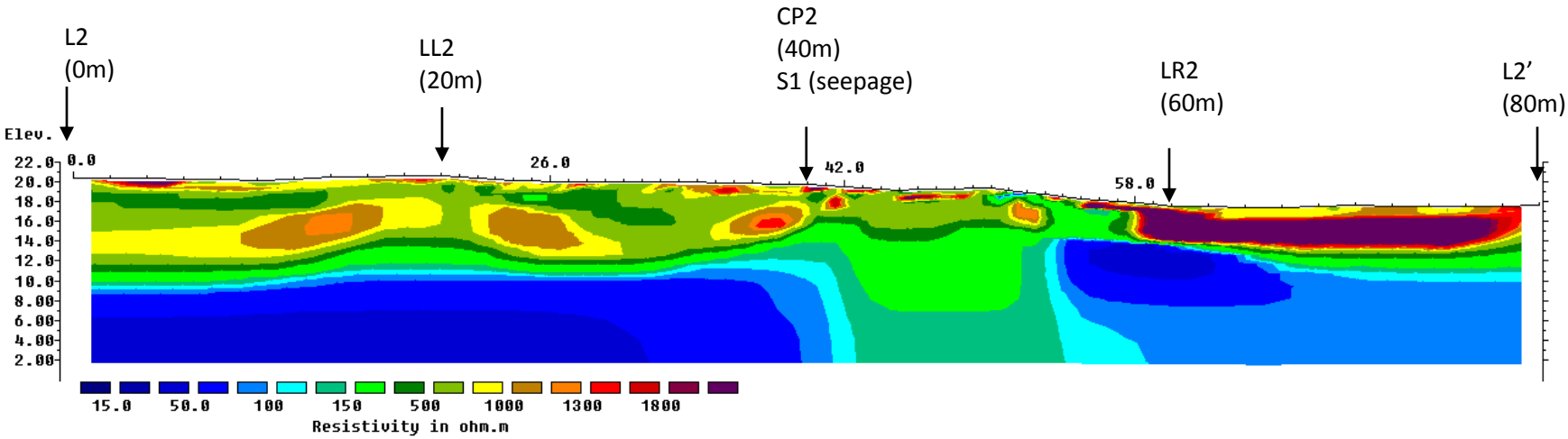

Figure 4.5: Subsurface image results by Electrical Resistivity method at line 2 (L2-L2')

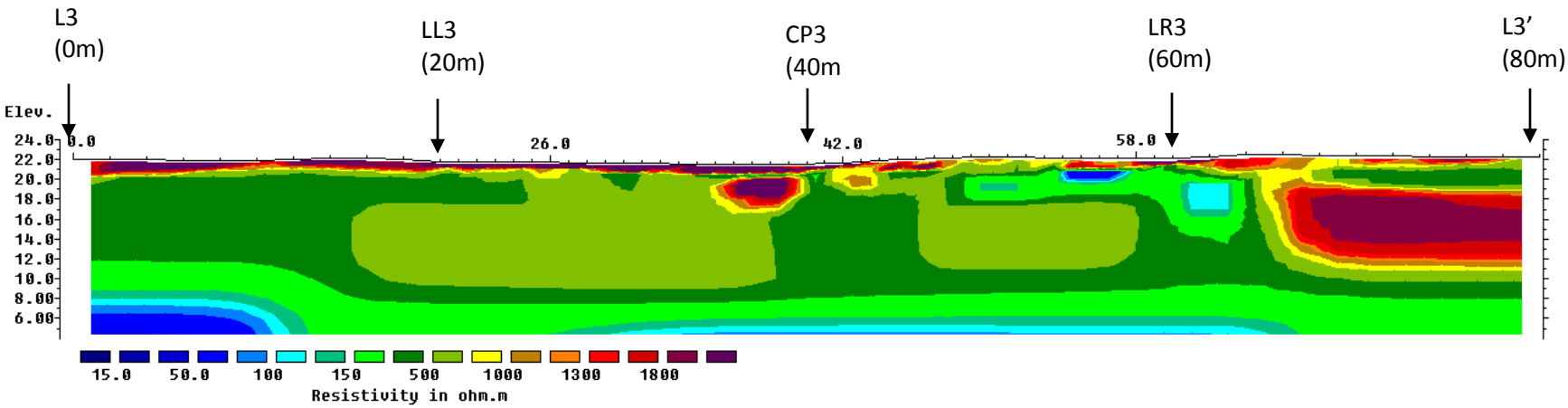

Figure 4.6: Subsurface image results by Electrical Resistivity method at line 3 (L3-L3')

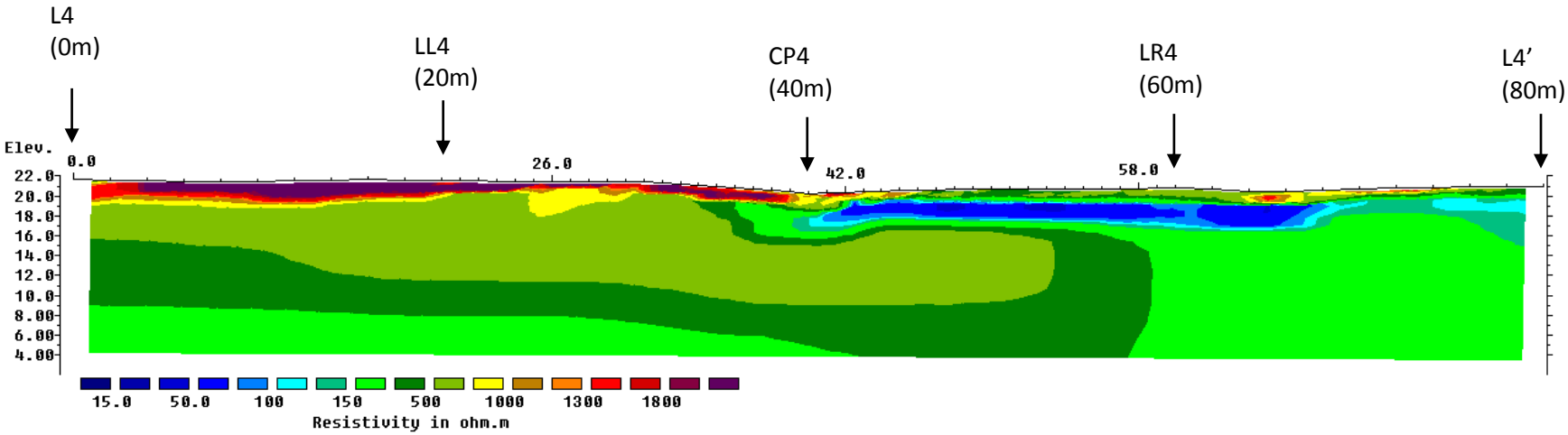

Figure 4.7: Subsurface image results by Electrical Resistivity method at line 4 (L4-L4')

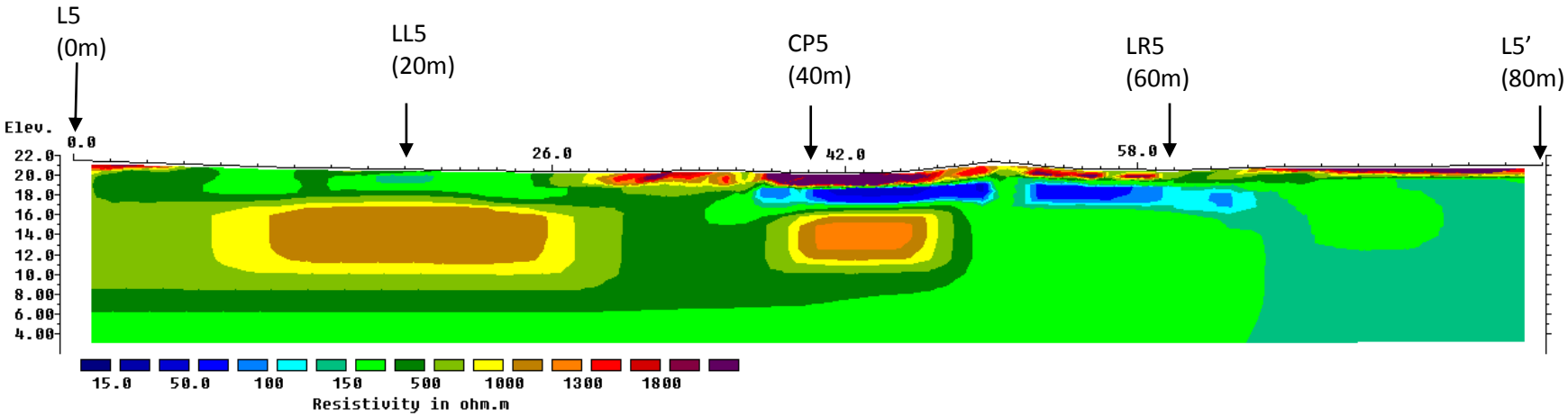

Figure 4.8: Subsurface image results by Electrical Resistivity method at line 5 (L5-L5')

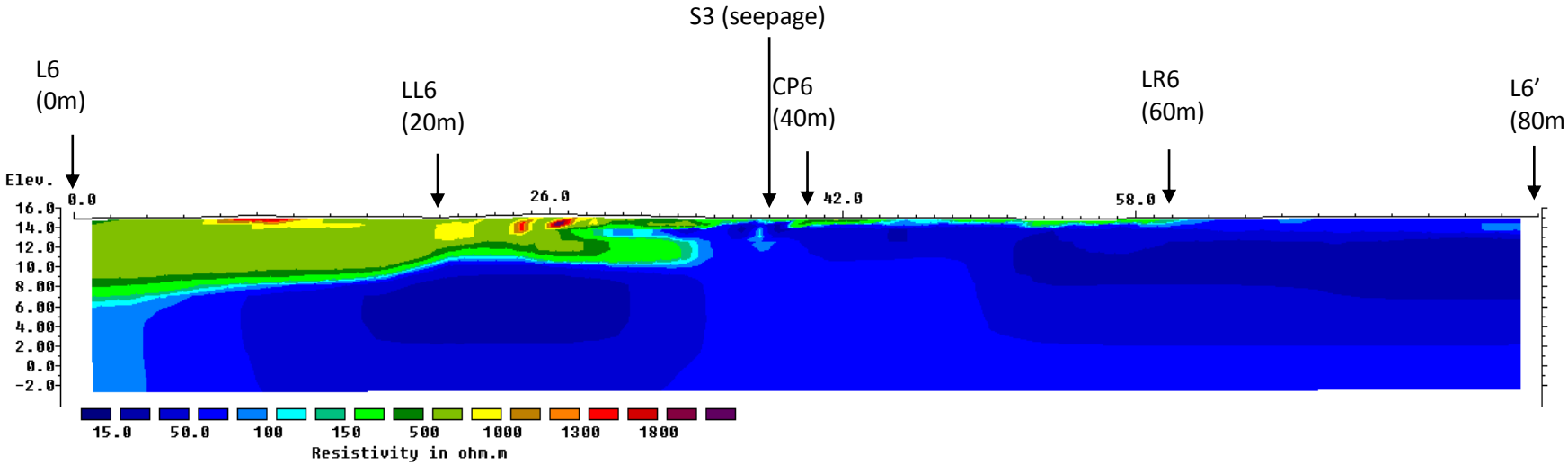

Figure 4.9: Subsurface image results by Electrical Resistivity method at line 6 (L6-L6')

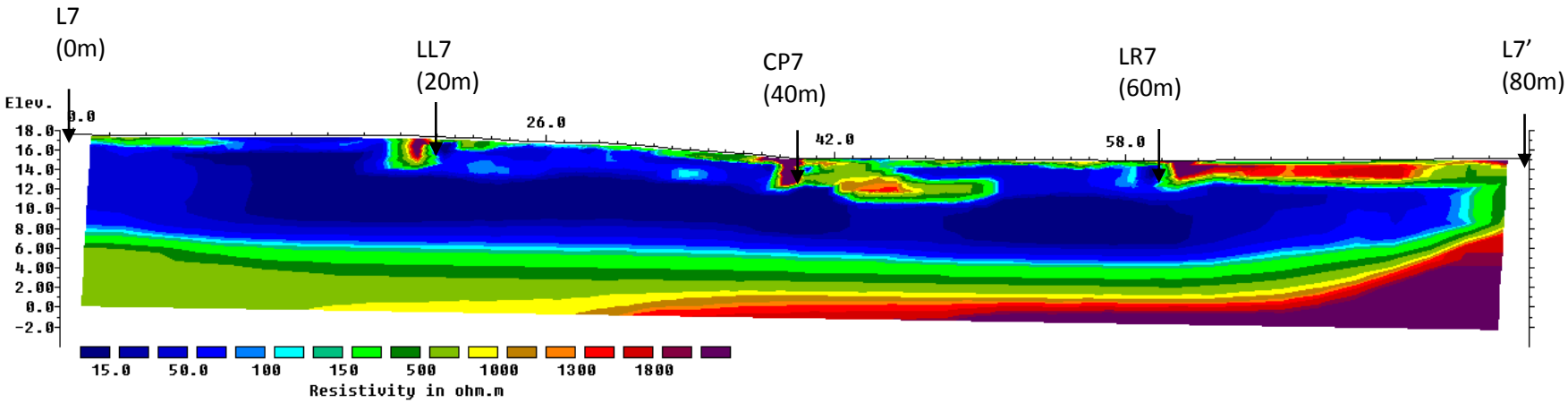

Figure 4.10: Subsurface image results by Electrical Resistivity method at line 7 (L7-L7')

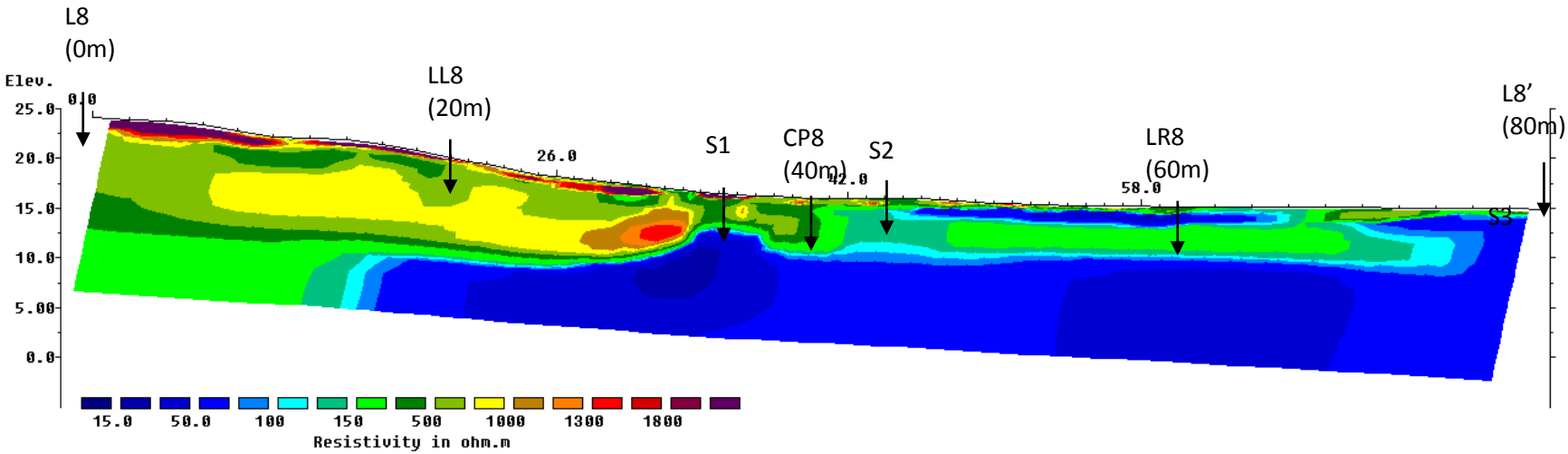

Figure 4.11: Subsurface image results by Electrical Resistivity method at line 8 (L8-L8')

4.8 Discussion and Conclusions

The 2-D resistivity images provided the important information of water seepage occurrence in this study area. The low resistivity value presence in this area indicated presence of permeable soil saturated with water. It was believed the presence of saturated water in dam embankment caused the problem of water seepage. Results from the 2D resistivity model reveal a dam seepage occurs at the back of embankment that may have been caused by several factors.

In conclusion, there are two possible causes of water seepage dams occur. First due to the high-pressure head subsequently induced high pore water pressure and the pressure is released at the seepage points especially in the boundary connection area between engineered material dam and natural material dam. The pressure results in collapsed and eroded soil block that occurs in the area resulting in seepage drainage. The second cause is due to excessive agriculture irrigation activity that acts from the surrounding of the embankment dam.

However, further investigation such as using borehole data may able to confirm in detail regarding the groundwater seepage from electrical resistivity method within this area. The propose remediation action can be used to overcome this problem. The remediation consists of groundwater withdrawal by constructing a few numbers of tube wells to reduce groundwater level within this area. ERM survey was applicable to be a good alternative method in shallow subsurface profiling due to its effective in terms of cost, time and quality provide. Furthermore, this method used a surface method during the data acquisition which enable the preservation of site destruction thus contributing to our sustainable environment.

4.9 List of References

Awni T. Batayneh, 2006. Use of electrical resistivity methods for detecting subsurface fresh and saline water and delineating their interfacial configuration: a case study of the eastern Dead Sea coastal aquifers, Jordan, Hydrogeology Journal, Volume 14: pp 1277–1283.

Daniels, F. and Alberty, R.A., (1996). Physical Chemistry. John Wiley and Sons, Inc.

Dey A. and Morrison H.F., 1979. Resistivity modelling for arbitrarily shaped two-dimensional structures. Geophysical Prospecting Volume 27, Issue 1, pp 106–136.

Flathe, H., 1976. The role of geological concept in geophysical research work for solving hydrogeological problems. Geoexploration 14, 195-206.

Jabatan Mineral dan Geosains (JMG), 1985. Peta Geologi Semenanjung Malaysia. Cetakan ke 8. Ketua Pengarah Jabatan Mineral dan Geosains Malaysia. Kementerian Sumber Asli dan Alam Sekitar.

Loke, M.H. and Barker R.D., 1995. Least-squares deconvolution of apparent resisitivity Pseudosections. Geophysics 60, 1682-1690.

Keller, G.V., and Frischknecht, F.C., (1996). Electrical Method In Geophysics Prospecting. Pergamon Press. Inc., Oxford. p. 517.

Loke, M.H. and Barker, R.D., 1996. Practical techniques for 3D resistivity surveys and data inversion. Geophysical Prospecting Volume 44, Number 3, pp 499-523. GPPRAR44(3)351-554(1996), ISSN 0016-8025.

Loke M.H and Barker R.D, 1996. Rapid least squares inversion of apparent resistivity pseudosection using a quasi-Newton method. Geophysical Prospecting, Volume 44, Number 3, 131–152. GPPRAR44(1)1-178(1996), ISSN 0016-8025.

Loke M.H., 2000. Electrical imaging surveys for environmental and engineering studies A practical guide to 2-D and 3-D surveys (Available online at www.geoelectrical.com/downloads.php). pp 1-60.

Loke, M.H., Acworth, I., and Dahlin, T. 2003. A comparison of smooth and blocky inversion methods in 2D electrical imaging surveys. Exploration Geophysics Volume 34, Issue 3, pp 182-187. (Available online at www.geoelectrical.com/downloads.php and email to mhloke@tm.net.my)

Mohd Hazreek Zainal Abidin, Rosli Saad, Fauziah Ahmad, Devapriya Chitral Wijeyesekera and Mohamad Faizal Tajul Baharuddin (2011) Application of Geophysical Methods in Civil Engineering. Malaysian Technical Universities International Conference on Engineering & Technology (MUiCET 2011)

Umar Hamzah, Rahman Yaacup, Abdul Rahim Samsudin and Mohd Shahid Ayub, 2006. Electrical imaging of the groundwater aquifer at Banting, Selangor, Malaysia, Environmental Geology 49, Issue 8, pp 1156–1162.

PHOTOS

L1-L1’

L2-L2'

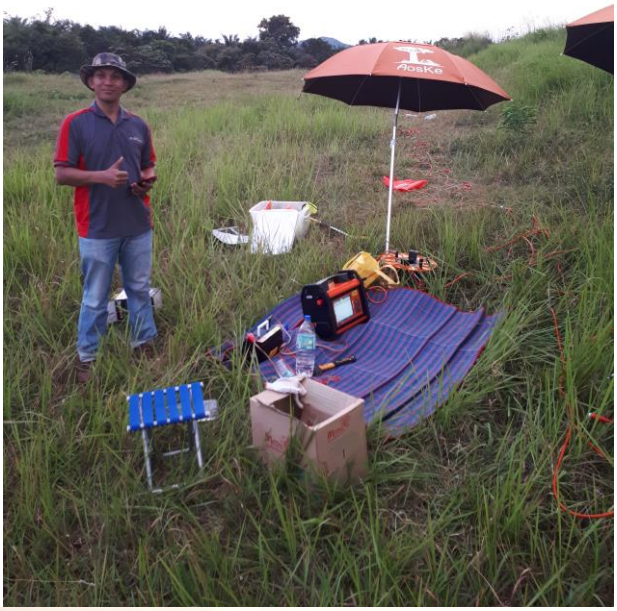

L3-L3’

L4-L4’

L5-L5’

L6-L6’

L7-L7'

L8-L8'

- **THE END -**